



Title	Identification of Jasmonic Acid and Jasmonoyl-Isoleucine, and Characterization of AOS, AOC, OPR and JAR1 in the Model Lycophyte <i>Selaginella moellendorffii</i>
Author(s)	Pratiwi, Putri; Tanaka, Genta; Takahashi, Tomohiro; Xie, Xiaonan; Yoneyama, Koichi; Matsuura, Hideyuki; Takahashi, Kosaku
Citation	Plant and Cell Physiology, 58(4), 789-801 <a href="https://doi.org/10.1093/pcp/pcx031">https://doi.org/10.1093/pcp/pcx031</a>
Issue Date	2017-04
Doc URL	<a href="http://hdl.handle.net/2115/68680">http://hdl.handle.net/2115/68680</a>
Rights	This is a pre-copyedited, author-produced PDF of an article accepted for publication in Plant & cell physiology following peer review. The version of record 58(4), pp789-801 is available online at: <a href="https://doi.org/10.1093/pcp/pcx031">https://doi.org/10.1093/pcp/pcx031</a>
Type	article (author version)
Additional Information	There are other files related to this item in HUSCAP. Check the above URL.
File Information	Manuscript20170215.pdf



[Instructions for use](#)

1   **Title and running head:**

2   Identification of Jasmonic Acid and Jasmonoyl-Isoleucine and Characterization of AOS, AOC,

3   OPR and JAR1 in the Model Lycophyte *Selaginella moellendorffii*

4

5   Identification of JA in *Selaginella moellendorffii*

6   –

7   **Corresponding author**

8   Dr. Kosaku Takahashi

9   Affiliation: Research Faculty of Agriculture, Hokkaido University

10   Address: Kita 9 Nishi 9, Kita-ku, Sapporo, 060-8589 Japan

11   Tel: +81-11-706-3349

12   Fax: +81-11-706-2505

13   E-mail: [kosaku@chem.agr.hokudai.ac.jp](mailto:kosaku@chem.agr.hokudai.ac.jp)

14

15   **Subject Areas:** (2) environmental and stress responses.

16   **Number of black and white figures:** 10.

17   **Number of tables:** 1.

18   **Number of supplemental materials:** 1.

19

20 **Title**

21 Identification of jasmonic acid and jasmonoyl-isoleucine and the characterization of AOS, AOC,  
22 OPR and JAR1 in the model lycophyte *Selaginella moellendorffii*

23

24 **Authors byline**

25 Putri Pratiwi<sup>1</sup>, Genta Tanaka<sup>1</sup>, Tomohiro Takahashi<sup>1</sup>, Xiaonan Xie<sup>2</sup>, Koichi Yoneyama<sup>2</sup>,  
26 Hideyuki Matsuura<sup>1</sup>, and Kosaku Takahashi<sup>1,\*</sup>

27

28 **Author's address**

29 <sup>1</sup>Research Faculty of Agriculture, Hokkaido University, Sapporo 060-8589, Japan

30 <sup>2</sup>Center for Bioscience Research and Education, Utsunomiya University, Utsunomiya 321-8505,  
31 Japan

32

33 **Abbreviation**

34 AOC, allene oxide cyclase; AOS, allene oxide synthase; COI1, coronatine insensitive 1; 12,13-  
35 EOT, (9Z,15Z)-(13S)-12,13-epoxyoctadeca-9,11,15-trienoic acid; GC-MS, gas chromatography-  
36 mass spectrometry; 13-HPOT, 13-hydroperoxyoctadecatrienoic acid; IPTG, isopropyl  $\beta$ -D-1-  
37 thiogalactopyranoside; JA, jasmonic acid; JA-Ile, jasmonoyl-isoleucine; JAR1, jasmonic acid  
38 resistant 1; JAZ, jasmonate-zim domain; LOX, lipoxygenase; Ni-NTA, nickel-nitrilotriacetic  
39 acid; OPC-8:0, 3-oxo-2-(*cis*-2'-pentenyl)cyclopentane-1-octanoic acid; OPDA, 12-oxo-  
40 phytodienoic acid; OPR, 12-oxo-phytodienoic acid reductase; SCF, skp-cullin-F box; SDS-  
41 PAGE, sodium dodecyl sulfate-polyacrylamide gel electrophoresis; UPLC-MS/MS, ultra-  
42 performance liquid chromatography-tandem mass spectrometry

43      **Abstract**

44      Jasmonic acid (JA) is involved in a variety of physiological responses in seed plants.  
45      However, the detection and role of JA in lycophytes, a group of seedless vascular plants, have  
46      remained elusive until recently. This study provides the first evidence of 12-oxo-phytodienoic  
47      acid (OPDA), JA, and jasmonoyl-isoleucine (JA-Ile) in the model lycophyte *Selaginella*  
48      *moellendorffii*. Mechanical wounding stimulated the accumulation of OPDA, JA, and JA-Ile.  
49      These data were corroborated by the detection of enzymatically active allene oxide synthase  
50      (AOS), allene oxide cyclase (AOC), 12-oxo-phytodienoic acid reductase 3 (OPR3), and JA-Ile  
51      synthase (JAR1) in *S. moellendorffii*. SmAOS2 is involved in the first committed step of JA  
52      biosynthesis. SmAOC1 is a crucial enzyme for generating the basic structure of jasmonates and is  
53      actively involved in the formation of OPDA. SmOPR5, a functionally active OPR3-like enzyme,  
54      is also vital for the reduction of (+)-*cis*-OPDA, the only isomer of the JA precursor. The  
55      conjugation of JA to Ile by SmJAR1 demonstrates that *S. moellendorffii* produces JA-Ile. Thus,  
56      the four active enzymes have characteristics similar to those in seed plants. Wounding and JA  
57      treatment induced the expression of *SmAOC1* and *SmOPR5*. Furthermore, JA inhibited the  
58      growth of shoots in *S. moellendorffii*, which suggests that JA functions as a signaling molecule in  
59      *S. moellendorffii*. This study proposes that JA evolved as a plant hormone for stress adaptation,  
60      beginning with the emergence of vascular plants.

61

62      **Keywords**

63      AOS; AOC; JAR1; Jasmonic acid; OPR3; *Selaginella moellendorffii*

64

65      **Introduction**

66      As sessile organisms, plants must adapt to many environmental stresses that can negatively  
67      affect their development, growth, productivity, and fertility by altering their physiological,  
68      morphological, and/or developmental processes. Many studies have found that JA modulates  
69      numerous plant physiological processes that are related to development and defense responses  
70      (Wasternack and Parthier 1997, Ziegler et al. 2000, Ishiguro et al. 2001, Wasternack 2007).  
71      Indeed, JA is a naturally occurring phytohormone that is ubiquitous in seed plant species  
72      (Creelman and Mullet 1997).

73      The JA biosynthetic pathway (Fig. 1) starts with the lipase-mediated release of  $\alpha$ -linolenic acid  
74      from the membrane lipids of chloroplasts (Wasternack and Hause 2013), which is triggered by  
75      abiotic and biotic stresses (Farmer and Ryan 1992, Mueller et al. 1993, Conconi et al. 1996,  
76      Penninckx et al. 1996, Narváez-Vásquez et al. 1999). In chloroplasts,  $\alpha$ -linolenic acid is  
77      converted into 13(S)-hydroperoxyoctadecatrienoic acid [13(S)-HPOT]; this process is mediated  
78      by 13-lipoxygenase (13-LOX). The 13(S)-HPOT intermediate can be dehydrated through the  
79      action of allene oxide synthase (AOS), which leads to JA biosynthesis (Yan et al. 2013). In the  
80      presence of AOS, the dehydration of the resultant fatty acid hydroperoxide forms an allene oxide  
81      (12,13-EOT), which is then cyclized by allene oxide cyclase (AOC) into *cis*-(+)-12-oxo-  
82      phytodienoic acid [(9S,13S)-OPDA]. The specificity of AOC determines the configuration of the  
83      side chains in the naturally occurring structure of jasmonates. The resulting OPDA is then  
84      transferred into peroxisomes, where OPDA reductase 3 (OPR3) reduces *cis*-(+)-OPDA to 3-oxo-  
85      2-(*cis*-2'-pentenyl)cyclopentane-1-octanoic acid (OPC-8:0), which is then converted into (+)-7-  
86      *iso*-JA through three  $\beta$ -oxidation steps. Subsequently, (+)-7-*iso*-JA is isomerized to (-)-JA and  
87      released into the cytoplasm via an unknown mechanism (Ziegler et al. 2000, Hyun et al. 2008,

88 Khan et al. 2012). JA can be enzymatically converted into many derivatives, such as methyl  
89 jasmonate and JA-amino acid conjugates. The jasmonic acid resistant 1 (*JARI*) gene encodes the  
90 enzyme that is responsible for the conjugation of JA to amino acids, i.e., isoleucine and valine.  
91 Among these conjugates, JA-Ile is considered to be an important compound in the JA signaling  
92 pathway (Stenzel et al. 2012). Under stress conditions, the JA-Ile level increases, and JA-Ile  
93 binds to its receptor, COI1, a component of the SCF complex. Subsequently, JA-Ile mediates the  
94 initial binding of the JAZ protein to the COI1-JA-Ile unit of the SCF complex, which results in  
95 degradation by the 26S proteasome and the release of MYC2 (Fonseca et al. 2009a, 2009b,  
96 Sheard et al. 2010, Santino et al. 2013).

97 Vascular plants have survived on earth for the past 420 million years and have diverged  
98 into several descendants. Only two descendants have survived: the euphyllophytes and  
99 lycophytes (Kenrick and Crane 1997, Banks et al. 2011). Fossil evidence shows that lycophytes  
100 diverged shortly after land plants evolved vascular tissues, which generated all other vascular  
101 plants. There are currently only three extant lycophyte groups: the Lycopodiales (club mosses),  
102 Isoetales (quillworts), and Selaginellales (spike mosses) (Weng et al. 2005, Banks 2009, Hecht et  
103 al. 2011). Recently, the approximately 100 Mbp genome of *Selaginella moellendorffii* was fully  
104 sequenced (Banks et al. 2011). This model lycophyte, as a representative of the earliest and still  
105 surviving vascular plant lineage, can potentially provide information for deciphering the  
106 evolution of the physiological, biochemical, and developmental processes that are unique to land  
107 plants.

108 The model plants that transitioned from water to land, such as the moss *Physcomitrella*  
109 *patens* and the liverwort *Marchantia polymorpha*, produce OPDA but not JA (Stumpe et al. 2010,  
110 Yamamoto et al. 2015). These findings strongly suggest that the first half of the octadecanoid

pathway in chloroplasts remains in bryophytes. Thereafter, the difference in JA production between seed plants and bryophytes is one of the significant observations in the study of plant evolution. The lycophytes are intermediate plants between bryophytes and seed plants, and this ancient lineage diverged shortly after land plants evolved vascular tissues. Thus, the origin of JA is of interest for studying plant evolution. In this study, we analyzed the lycophyte model *S. moellendorffii* to determine the presence of OPDA, JA, and JA-Ile, as well as the enzymatic activities of AOS, AOC, OPR3, and JAR1, which are involved in the biosynthesis of jasmonates. Moreover, we showed the growth inhibitory activity of OPDA, JA, and JA-Ile in *S. moellendorffii*. These data indicate a possible role for JA as a signaling molecule that regulates growth and response to wounding in *S. moellendorffii*.

121

## 122 Results

### 123 Identification of OPDA, JA, and JA-Ile in *S. moellendorffii*

124 Seed plants can biosynthesize JA and JA-Ile; however, these compounds are absent in the model  
125 bryophytes *P. patens* and *M. polymorpha* (Stumpe et al. 2010, Yamamoto et al. 2015). In this  
126 study, we evaluated *S. moellendorffii*, which belongs to a lycophyte group that is taxonomically  
127 positioned between bryophytes and euphylophytes, to identify JA and its related compounds. We  
128 detected OPDA, JA, and JA-Ile in *S. moellendorffii* using ultra-performance liquid  
129 chromatography tandem mass-spectrometry (UPLC-MS/MS) analysis (Fig. 2). The OPDA  
130 analytical data revealed a predominant peak in the chromatogram of an *S. moellendorffii* extract  
131 ( $m/z$  164.99 derived from the peak at  $m/z$  291.37 [M-H] $^-$ ; Figs. 2A, 2B, and 2C). This peak  
132 overlapped with the *cis*-OPDA standard peak, which indicates that OPDA is present in *S.*  
133 *moellendorffii*. The minor peak that eluted before *cis*-OPDA was speculated to be either an

134 unidentified OPDA-related compound or a *trans*-isomer of OPDA (Fig. 2B). The analytical JA  
135 data clearly demonstrated that the standard JA peak overlapped with the peak derived from an  
136 extract of *S. moellendorffii* (*m/z* 58.71 derived from the peak at *m/z* 209.09 [M–H]<sup>–</sup>; Figs. 2D, 2E,  
137 and 2F). This result indicated the presence of JA in *S. moellendorffii*. Furthermore, an analysis of  
138 JA-Ile showed that the retention time of standard JA-Ile was the same as that of the peak derived  
139 from an extract of *S. moellendorffii* (*m/z* 129.68 derived from the peak at *m/z* 323.03 [M–H]<sup>–</sup>;  
140 Figs. 2G, 2H, and 2I), suggesting that *S. moellendorffii* also biosynthesizes JA-Ile. The minor  
141 peak that was detected in the extract is potentially an unidentified contaminant that was not  
142 further analyzed (Fig. 2H). These data are the first evidence of OPDA, JA, and JA-Ile in *S.*  
143 *moellendorffii*.

144

145 *Accumulation of OPDA, JA, and JA-Ile upon wounding stress*

146 JA plays important roles in stress adaptation. Therefore, the accumulation of JA is considered  
147 a response to adverse environmental conditions involving both biotic and abiotic stresses,  
148 especially in seed plants (Wasternack and Hause 2013). Wounding activates the octadecanoid  
149 pathway, which results in the accumulation of OPDA, JA, and JA-Ile in seed plants. To illustrate  
150 the response of *S. moellendorffii* to wounding stress, the photosynthesizing organs (stems and  
151 microphylls) were mechanically wounded and then analyzed at different time points. The  
152 endogenous levels of OPDA, JA, and JA-Ile were analyzed using UPLC-MS/MS (Fig. 3). *S.*  
153 *moellendorffii* transiently produced a high level of OPDA within the first 10 min after wounding.  
154 OPDA was approximately 200-fold more abundant than JA at 10 min after wounding, whereas  
155 the JA level peaked at 30 min, following the initial increase at 10 min. In contrast to the rapid  
156 increase in the OPDA and JA concentrations, JA-Ile accumulation was delayed and started at 180

157 min after wounding. The increased levels of JA and JA-Ile were accompanied by a rapid decrease  
158 in the OPDA concentration. These data revealed that wounding increased the endogenous levels  
159 of these jasmonates in *S. moellendorffii*, similar to the response in seed plants. Accordingly,  
160 environmental stress probably activates the octadecanoid pathway. OPDA, JA, and JA-Ile also  
161 seem to play a role in regulating the response to wounding in *S. moellendorffii*.

162

163 *Putative AOS, AOC, OPR3 and JAR1 genes in S. moellendorffii*

164 To further confirm the presence of OPDA, JA, and JA-Ile in *S. moellendorffii*, we  
165 investigated the characteristics of important JA biosynthetic enzymes in *S. moellendorffii*. A  
166 genomic database analysis using Phytozome v 11.0  
167 (<https://phytozome.jgi.doe.gov/pz/portal.html>) was performed to screen *AOS*, *AOC*, *OPR3*, and  
168 *JAR1* homologous genes in *S. moellendorffii* using *Arabidopsis* amino acid sequences  
169 corresponding to these proteins as queries. As a result, the presence of putative *AOS* (*SmAOS1*,  
170 *Sm\_271334*; *SmAOS2*, *Sm\_177201*; *SmAOS3*, *Sm\_228572*), *AOC* (*SmAOCl*, *Sm\_91887*), *OPR3*  
171 (*SmOPR1*, *Sm\_270843*; *SmOPR5*, *Sm\_111662*), and *JAR1* (*SmJAR1*, *Sm\_110439*) genes was  
172 predicted in *S. moellendorffii* (Supplementary Table S1).

173

174 *Functional analysis of SmAOS2*

175 The first committed step of JA biosynthesis is catalyzed by AOS, which converts 13-HPOPT  
176 into unstable 12,13-EOT. A genomic database analysis of Phytozome v 11.0 revealed the  
177 presence of nine putative *AOS* genes in *S. moellendorffii*. Amino acid sequence analysis of the  
178 SmAOS candidates showed that SmAOS1, SmAOS2, and SmAOS3 were promising candidates  
179 containing the important sequence motifs: the I-helix GXXX (F/L), EXLR motif, and heme-

180 binding PXVXNKQCPG, which are characteristic of members of the CYP74 family  
181 (Supplementary Fig. S1) (Koeduka et al. 2015). Additionally, the amino acid sequences of  
182 SmAOS1, SmAOS2, and SmAOS3 are quite similar (Supplementary Fig. S1). A phylogenetic  
183 tree of the AOSs showed that the SmAOSs were separated from the seed plant AOSs  
184 (Supplementary Fig. S2). Computational analysis using ChloroP v 1.1  
185 (<http://www.cbs.dtu.dk/services/ChloroP/>) and iPSORT (<http://ipsort.hgc.jp/>) for subcellular  
186 localization predicted the absence of a transit peptide in SmAOS1, SmAOS2, and SmAOS3,  
187 whereas most known AOSs are localized in chloroplasts (Schaller and Stintzi 2009).

188 To confirm AOS activity in this plant, the production of these recombinant SmAOSs was  
189 attempted. However, only recombinant SmAOS2 fused with a His-tag was successfully  
190 synthesized in *E. coli*. Purification of recombinant SmAOS2 by Ni-NTA affinity column  
191 chromatography and SDS-PAGE analysis revealed a clear band of SmAOS2 with an expected  
192 molecular weight of approximately 50 kDa (Supplementary Fig. S3). The AOS reaction converts  
193 13(S)-HPOT to unstable 12,13-EOT, which is non-enzymatically changed to racemic OPDA.  
194 Therefore, AOS enzymatic activity can be determined by analyzing the presence of racemic  
195 OPDA. The recombinant SmAOS2 was incubated with 13(S)-HPOT, and then the products were  
196 extracted with ethyl acetate, followed by isomerization by alkaline treatment and methylation  
197 using ethereal diazomethane. Laudert et al. (1997) demonstrated that chiral GC-MS analysis of  
198 methylated OPDA can clearly separate the *trans*-isomers of methylated OPDA; therefore,  
199 isomerization was performed to convert *cis*-OPDA to *trans*-OPDA. Peaks of methylated (+)-  
200 *trans*-OPDA and methylated (-)-*trans*-OPDA were both identified in the SmAOS2 reaction  
201 products on the chiral GC-MS chromatogram (Fig. 4). Furthermore, an ion peak at *m/z* 306,  
202 corresponding to the molecular ion peak [M]<sup>+</sup> of OPDA methyl ester, was observed together with

203 unique fragment ion peaks at  $m/z$  275 ( $[M-OCH_3]^+$ ),  $m/z$  238 ( $[M-C_5H_9]^+$ ), and  $m/z$  149  
204 ( $[M-C_9H_{17}O_2]^+$ ) in the GC-MS spectral data of both methylated (+)-*trans*-OPDA and methylated  
205 (-)-*trans*-OPDA (Supplementary Figs. S4S6, Laudert et al. 1997). These results showed that  
206 SmAOS2 had AOS activity similar to that of previously characterized AOSs.

207

208 *Functional analysis of SmAOC1*

209 *AOC* has been successfully cloned from seed plants, a moss, and a liverwort (Ziegler et al.  
210 2000, Agrawal et al. 2003, Stenzel et al. 2003, Maucher et al. 2004, Farmaki et al. 2007, Pi et al.  
211 2008, Stumpe et al. 2010, Hashimoto et al. 2011, Yamamoto et al. 2015). The 5'-UTR of  
212 *SmAOC1* was examined by 5'-RACE to obtain the full-length sequence. A computational  
213 analysis using ChloroP v 1.1 and iPSORT predicted that SmAOC1 has a chloroplast transit  
214 peptide at its N-terminus. The amino acid sequence alignment of SmAOC1 and AOCs of other  
215 plants showed that SmAOC1 had high similarity to other AOCs (Supplementary Fig. S7). The  
216 phylogenetic tree of AOCs demonstrated that SmAOC1 was related to MpAOC from the  
217 liverwort *M. polymorpha* and to AOCs in seed plants, while it was separated from PpAOC1 and  
218 PpAOC2 of the moss *P. patens* (Supplementary Fig. S8).

219 To determine whether SmAOC1 is involved in the production of OPDA, *SmAOC1* was  
220 cloned and overexpressed in *E. coli*. The recombinant SmAOC1 was fused with a His-tag at the  
221 N-terminus to replace the chloroplast signal peptide. After purifying SmAOC1 using Ni-NTA  
222 affinity column chromatography, a protein with the expected size of 22 kDa was clearly detected  
223 as a single band by SDS-PAGE analysis (Supplementary Fig. S3). The purified recombinant  
224 SmAOC1 was used for enzymatic analysis.

225 Due to the instability of 12,13-EOT, which is the substrate for the AOC reaction, the  
226 enzymatic activity of SmAOC1 was tested in a reaction mixture containing SmAOC1, PpAOS1,  
227 and 13(S)-HPOT as substrates. For a negative control, only PpAOS1 and 13(S)-HPOT were used  
228 in a reaction mixture. After terminating the reaction, the resulting *cis*-OPDA product was  
229 converted to *trans*-OPDA by alkaline treatment, which was followed by methylation using  
230 ethereal diazomethane. *Trans*-OPDA was finally analyzed by chiral GC-MS. The molecular ion  
231 peak of the OPDA methyl ester at *m/z* 306 [M]<sup>+</sup> was monitored to evaluate SmAOC1 activity  
232 (Laudert et al. 1997) (Fig. 5). The GC-MS analysis showed a predominant molecular ion peak (ca.  
233 97%) in the reaction mixture containing SmAOC1. The retention time of this peak coincided with  
234 the standard *trans*-(+)-OPDA methyl ester, which represents *cis*-(+)-OPDA. In contrast, two  
235 molecular ion peaks of the racemic *trans*-OPDA methyl esters were detected in the product of the  
236 PpAOS1 reaction. This result demonstrated that SmAOC1 converts 12,13-EOT into *cis*-(+)-  
237 OPDA, similar to previously reported AOCs.

238 The first of three enzymes involved in JA biosynthesis (LOX, AOS, and AOC) have been  
239 reported to reside in chloroplasts (Schaller and Stintzi, 2009). To examine whether SmAOC1 is  
240 localized in chloroplasts, a 35S::SmAOC1-GFP plasmid was constructed and introduced into *P.*  
241 *patens* protoplasts and was then finally observed by confocal laser scanning microscopy. The  
242 green fluorescent signal of SmAOC1 fused with GFP was clearly identified by the red auto-  
243 fluorescence of chlorophyll. The overlay data also strongly supported that SmAOC1 is located in  
244 chloroplasts, which is similar to the other characterized AOCs (Supplementary Fig. S9).  
245 Accordingly, chloroplast could be the functional organelle in the biosynthesis of OPDA in *S.*  
246 *moellendorffii*.

247

248     *Functional analysis of SmOPRs*

249     OPRs are classified into two groups based on their ability to reduce OPDA: OPR3-like  
250     enzymes (e.g., *Arabidopsis* AtOPR3, tomato SIOPR3, and rice OsOPR7) and OPR1-like enzymes  
251     (e.g., AtOPR1 and SIOPR1) (Breithaupt et al. 2009). OPR3-like enzymes catalyze the reduction  
252     of *cis*-(+)-OPDA, a natural JA precursor, and of *cis*-(-)-OPDA, which is not involved in JA  
253     biosynthesis. The *Arabidopsis opr3* mutant shows male sterility and is desensitized to responses  
254     involving JA signaling. In contrast, OPR1-like enzymes preferentially reduce *cis*-(-)-OPDA  
255     rather than *cis*-(+)-OPDA; therefore, OPR1-like enzymes might function in pathways other than  
256     JA biosynthesis.

257     A genomic database search using Phytozome v 11.0 predicted the presence of six putative  
258     OPR genes in *S. moellendorffii*. All of the amino acid sequences of candidate SmOPRs were  
259     aligned with those of other known OPRs (Supplementary Fig. S10). Based on a comparison of  
260     two critical amino acids for substrate binding and a phylogenetic analysis of SmOPRs  
261     (Supplementary Fig. S10), two genes designated *SmOPR1* and *SmOPR5* were highly promising  
262     candidate genes that encoded OPR3-like enzymes involved in JA biosynthesis. SmOPR1 harbors  
263     two important active-site residues, Phe and His, as an OPR3 motif in the active site, which is  
264     considered to be necessary to reduce the JA precursor *cis*-(+)-OPDA. However, SmOPR1 was  
265     grouped with the other SmOPRs in an independent OPR cluster (Supplementary Fig. S11). In  
266     contrast, SmOPR5 was a member of the cluster of OPR3-like enzymes, such as AtOPR3,  
267     OsOPR7, SIOPR3, ZmOPR7, and ZmOPR8, which are active in JA biosynthesis (Supplementary  
268     Fig. S11). Moreover, SmOPR5 shared 53% amino acid sequence identity with AtOPR3.  
269     Nonetheless, instead of Phe and His, which are considered unique to the OPR3 substrate filter,

270 the active site residues of SmOPR5 were Trp and His. Therefore, these two genes were selected  
271 for further analysis to verify their enzymatic activity.

272 To confirm the enzymatic activities, recombinant SmOPR1 and SmOPR5 proteins fused with  
273 a His-tag were produced in *E. coli*. SDS-PAGE analysis showed that the recombinant SmOPR1  
274 and SmOPR5 appeared as single bands with an expected molecular weight of approximately 40  
275 kDa (Supplementary Fig. S3). The enzymatic reactions were conducted according to the method  
276 of Schaller et al. (1998) with some modifications. Recombinant SmOPR1 and SmOPR5 were  
277 incubated in 50 mM potassium phosphate buffer (pH 7.4) containing NADPH and *cis*-( $\pm$ )-OPDA.  
278 After terminating the OPR reactions, the *cis*-isomers of OPDA and OPC-8:0 in the OPR reaction  
279 solutions were converted into *trans*-isomers of OPDA and OPC-8:0 by alkaline treatment. The  
280 reaction products were finally analyzed by chiral GC-MS after methylation (Vick and  
281 Zimmerman 1983, Laudert et al. 1997). In the GC-MS chromatogram of SmOPR1 reaction  
282 products, only the peak of methylated *trans*-(-)-OPC-8:0, which was derived from the non-JA  
283 precursor *cis*-(-)-OPC-8:0, appeared; there was no peak for methylated *trans*-(+)-OPC-8:0, which  
284 was derived from *cis*-(+)-OPDA, a natural JA biosynthetic intermediate (Fig. 6). Therefore,  
285 SmOPR1 did not participate in JA biosynthesis. In contrast, SmOPR5 catalyzed the reduction of  
286 both *cis*-( $\pm$ )-OPDA enantiomers to both ( $\pm$ )-OPC-8:0 enantiomers (Fig. 6). The fragmentation of  
287 methylated *trans*-(+)-OPC-8:0 (Peak 1) derived from *cis*-(+)-OPDA was similar to that of  
288 standard methylated OPC-8:0 (Supplementary Figs. S12 and S13). These data indicated that  
289 *SmOPR5* encodes a functional OPR3 that participates in JA biosynthesis in *S. moellendorffii*.

290

291 *Enzymatic production of JA-Ile by SmJARI*

JA-Ile is a versatile signaling molecule for JA-mediated defense and developmental events and is produced by the conjugation of JA and Ile. JAR1s are GH3 proteins that have the ability to synthesize JA-Ile (Staswick and Tiryaki 2004). An *Arabidopsis jar1* mutant, which is unable to produce JA-Ile, fails to trigger JA-mediated responses (Suza and Staswick 2008). Thus, JAR1 activity is necessary for JA signal transduction in seed plants. Here, we found 14 *JAR1* homologous genes in the Phytozome database using AtJAR1 as a query (Supplementary Table S1). Multiple sequence alignment and phylogenetic analysis using Clustal Omega software were performed to show the relationship between these JAR1 homologous proteins in *S. moellendorffii* and the other existing JAR1 proteins (Supplementary Figs. S14 and S15). As a result, the candidate Sm\_110439, which was designated SmJAR1, was most closely related to AtJAR1, OsJAR1 and OsJAR2, which can synthesize JA-Ile (Staswick and Tiryaki 2004, Wakuta et al. 2011). Moreover, SmJAR1 also has three short conserved motifs involved in ATP/AMP binding (Chang et al. 1997): SSGTSQGRPK (motif 1), YGSSE (motif 2), and YRLGD (motif 3) (Supplementary Fig. S14). To determine whether *SmJAR1* encodes functional JA-Ile synthase in *S. moellendorffii*, *SmJAR1* was isolated to check its enzymatic activity.

To evaluate JAR1 activity, *E. coli* expressing *SmJAR1* were incubated with (-)-JA as a substrate. JA-Ile in the culture supernatant of *E. coli* was analyzed by UPLC-MS/MS. The analytical data clearly showed that SmJAR1 catalyzes the conjugation of JA to Ile using endogenous ATP and Ile in *E. coli* (Fig. 7). To investigate the substrate specificity of SmJAR1, the conjugation of JA to other amino acids was also analyzed. No peak derived from another conjugate of JA-Trp, JA-Phe, or JA-Val appeared in the culture supernatant of *E. coli* expressing *SmJAR1* (Supplementary Fig. S16). Therefore, SmJAR1 was hypothesized to prefer Ile for conjugation with JA.

315

316     *Expression of genes encoding key enzymes in JA-Ile biosynthesis under wounding stress and JA*  
317     *treatment*

318       Wounding and JA induce the expression of a wide variety of genes in seed plants, such as  
319       defense-related genes, and genes encoding enzymes involved in JA biosynthesis. To determine if  
320       wounding and JA treatment affect gene expression in *S. moellendorffii*, quantitative RT-PCR  
321       analysis was performed to analyze the expression of *SmAOC1*, *SmOPR5*, and *SmJAR1*.  
322       Wounding increased the transcription levels of *SmAOC1*, *SmOPR5*, and *SmJAR1* (Fig. 8). The  
323       expression of *SmAOC1* was transiently induced at 10 min after wounding and then decreased  
324       until 180 min. The accumulation of *SmOPR5* mRNA reached a maximum 20 min after wounding  
325       and decreased thereafter. By contrast, only weak expression was observed for *SmJAR1* until 60  
326       min, followed by an increase in *SmJAR1* expression at 180 min. These results indicate that the  
327       expression kinetics of *SmAOC1*, *SmOPR5*, and *SmJAR1* coincided with the accumulation profiles  
328       of OPDA, JA, and JA-Ile in wounded *S. moellendorffii*.

329       The analytical data on *SmAOC1* and *SmOPR5* expression in JA-treated *S. moellendorffii*  
330       revealed an initial increase in transcription levels in the first 30 and 10 min, respectively, after JA  
331       treatment (Fig. 9). The accumulation of *SmAOC1* continued to increase until 60 min after JA  
332       application and decreased thereafter, whereas the transcription level of *SmOPR5* decreased 30  
333       min after treatment. The expression profiles of *SmAOC1* and *SmOPR5* in the plants treated with  
334       JA were similar to those in the wounded plants. In contrast to *SmAOC1* and *SmOPR5*, the  
335       expression of *SmJAR1* was suppressed within 10 min after JA treatment and remained at a low  
336       level thereafter.

337

338 *Effect of exogenous OPDA, JA, and JA-Ile on the growth of S. moellendorffii shoots*

339       Growth inhibition caused by JA is one of the most significant physiological responses in seed  
340 plants. To examine the ability of OPDA, JA, and JA-Ile to inhibit the growth of *S. moellendorffii*,  
341 bulbils of *S. moellendorffii* (Supplementary Fig. S17) were sprinkled onto soil, and the  
342 germinated plants were grown with or without treatment with OPDA, JA, or JA-Ile at  
343 concentrations of 25, 50, and 100  $\mu\text{M}$ . After four weeks, the lengths of the shoots of *S.*  
344 *moellendorffii* were measured. All jasmonates tested in this study were shown to have growth  
345 inhibitory effects on shoots of *S. moellendorffii* (Fig. 10, supplementary Fig. 18). Both OPDA  
346 and JA inhibited growth in a dose-dependent manner, with a stronger effect with OPDA than  
347 with JA. JA-Ile also retarded the growth of the shoots of this plant, but the growth inhibitory  
348 effect did not increase with increasing concentrations of JA-Ile. This is the first report that OPDA,  
349 JA, and JA-Ile inhibit the growth of seedless vascular plants, such as lycophytes.

350

351 **Discussion**

352 *Identification and accumulation of OPDA, JA, and JA-Ile*

353       In this study, the presence of OPDA, JA, and JA-Ile in *S. moellendorffii* was successfully  
354 demonstrated (Fig. 2). Moreover, wounding transiently increased the endogenous concentrations  
355 of OPDA and JA in *S. moellendorffii* within 10 min (Fig. 3), which is probably due to the role of  
356 jasmonates in regulating responses to environmental stress in *S. moellendorffii*. Given that  
357 wounding also stimulated OPDA and JA in the fern *Pteridium aquilinum* (Radhika et al. 2012),  
358 the accumulation of JA in response to wounding is likely a common physiological response  
359 among all vascular plant species (Maucher et al. 2004). However, JA-Ile accumulated more  
360 slowly than OPDA and JA after wounding. It is possible that the early rise in JA levels within 30

361 min represents an early response, whereas the slow JA-Ile accumulation may be attributable to a  
362 late stress response in this plant.

363 The transient increases in JA and OPDA after wounding observed in *S. moellendorffii* are  
364 similar to those observed in seed plants. It has been suggested that another metabolic pathway is  
365 required to inactivate JA responses in *S. moellendorffii*. In *Arabidopsis*, the oxidation of JA-Ile,  
366 which decreases the JA-Ile concentration, is important for regulating JA activity (Kitaoka et al.  
367 2011, Koo et al. 2011). A phylogenetic analysis of cytochrome P450s in *A. thaliana*, *P. patens*,  
368 and *S. moellendorffii* revealed that SmCYP94Js (SmCYP94J1, SmCYP94J2, SmCYP94J3,  
369 SmCYP94J5Pv1, and SmCYP94J5Pv2) are members of a cluster that includes AtCYP94B3 and  
370 AtCYP94C1 as enzymes responsible for the oxidation of JA-Ile and 12OH-JA-Ile (Banks et al.  
371 2011). SmCYP94Js are likely related to the oxidation of JA-Ile, leading to the inactivation of JA  
372 activity.

373 In studies of *P. patens* and *M. polymorpha*, only OPDA has been detected in both plants  
374 (Stumpe et al. 2010, Yamamoto et al. 2015). In contrast to vascular plants, JA is not important for  
375 the physiology of these model bryophytes. Hence, our data suggest that JA and JA-Ile  
376 biosynthesis first appeared after bryophytes in plant evolution (Figs. 2 and 3). Additionally, there  
377 is a significant difference between bryophytes and lycophytes. Lycophytes have a vascular  
378 system for the efficient transport of water, nutrients, and molecules, as well as for enhancing  
379 plant height and size. It is likely that the emergence of the JA biosynthetic pathway after OPDA  
380 is related to the acquisition by plants of a vascular system.

381

382 *Enzymatic activity*

383 There have been no previous studies on enzymes in the JA biosynthetic pathway of non-seed  
384 vascular plants. To support the analytical data showing the presence of OPDA, JA, and JA-Ile,  
385 the enzymatic activities of AOS, AOC, OPR3, and JAR1 were investigated. Here, genes  
386 encoding functional AOS, AOC, OPR3, and JAR1 proteins (SmAOS2, SmAOC1, SmOPR1 and  
387 SmOPR5, and SmJAR1, respectively) were identified in *S. moellendorffii*.

388

389 *SmAOS2*. The AOS reaction is the first committed step of JA biosynthesis in plants. AOS is  
390 classified as a member of the CYP74 family and requires an oxygenated fatty acid hydroperoxide  
391 substrate instead of oxygen or a redox partner (Howe and Schilmiller 2002, Werck-Reichhart et  
392 al. 2002). This study revealed three AOS candidate genes (*SmAOS1*, *SmAOS2*, and *SmAOS3*) in *S.*  
393 *moellendorffii* (Supplementary Figs. S1 and S2). Among them, recombinant SmAOS2, which  
394 was successfully produced in *E. coli*, exhibited AOS activity similar to that of previously  
395 reported AOSs (Fig. 4, Supplementary Figs. S4–S6). Computer programs analyzing protein  
396 subcellular localization did not predict a transit peptide in the N-terminus of SmAOS2. Because  
397 most known AOSs are localized in chloroplasts, SmAOS2 is likely located in chloroplasts for JA  
398 biosynthesis. Since the amino acid sequences of SmAOS1, SmAOS2, and SmAOS3 are similar,  
399 further investigation is needed to clarify the physiological functions of each of these SmAOSs.

400

401 *SmAOC1*. AOC is a critical enzyme that establishes the enantiomeric structure of OPDA, which  
402 contributes to the basic structure of jasmonates. The enzymatic activity of SmAOC1 is required  
403 for the synthesis of naturally occurring OPDA (Fig. 5). The stereochemistry of OPDA in *S.*  
404 *moellendorffii* is the same as that in other studied plants. Our microscopic observations using  
405 SmAOC1 fused to GFP showed that SmAOC1 localized to chloroplasts (Supplementary Fig. S9).

406 These results suggest that the first half of the octadecanoid pathway for synthesizing OPDA is  
407 present in the chloroplasts of *S. moellendorffii*. The presence of LOX, AOS, and AOC in  
408 chloroplasts may have been conserved during the process of land plant evolution.

409

410 *SmOPR1 and SmOPR5*. The enzymatic analysis of SmOPR1 and SmOPR5 revealed that *S.*  
411 *moellendorffii* possesses two types of OPRs that are classified by substrate preference: OPR1-like  
412 enzymes and OPR3-like enzymes. SmOPR1 and SmOPR5 are similar in their molecular mass  
413 and isoelectric point (pI) (Table 1) but differ in their substrate specificity for *cis*-OPDA isomers.  
414 Of these two SmOPRs, only SmOPR5 reduced *cis*-(±)-OPDA, including the endogenous  
415 substrate *cis*-(+)-OPDA, which is the natural JA precursor (Fig. 6, Supplementary Figs. S12 and  
416 S13). In contrast to SmOPR5, SmOPR1 reduced only *cis*-(−)-OPDA, which is the unnatural type  
417 (Fig. 6). SmOPR1 might instead be required for the oxylipin metabolic pathway.

418 A structural comparison of tomato SIOPR1 and SIOPR3 indicated that two active site  
419 residues, Tyr78 and Tyr246 in SIOPR1 and Phe74 and His244 in SIOPR3, are critical for  
420 substrate specificity (Breithaupt et al. 2009). SIOPR3 is less enantioselective due to its two  
421 relatively smaller amino acid residues that form a larger substrate binding pocket. In contrast, the  
422 relatively larger amino acids (two Tyr residues) in SIOPR1 permit access to only *cis*-(−)-OPDA,  
423 the unnatural type, at the substrate binding site. This study showed that SmOPR5, but not  
424 SmOPR1, actively converts the endogenous substrate *cis*-(+)-OPDA to *cis*-(+)-OPC-8:0. This  
425 result contrasts with the prediction from the substrate preference analysis of their active site  
426 residues but agrees with the phylogenetic analysis of OPRs (Supplementary Figs. S10 and S11).  
427 Mutation of the important amino acids Phe and His into Tyr in SIOPR3 did not completely  
428 change the substrate specificity (Breithaupt et al. 2009). There is an unidentified factor in the

429 structure of OPRs that is important for substrate specificity, and this factor must be identified by  
430 further crystal structure analysis.

431 Li et al. (2009) showed that OPRs from the lower land plants *P. patens* (PpOPR1, PpOPR2,  
432 PpOPR4, and PpOPR5) and *S. moellendorffii* (SmOPR1, SmOPR2, SmOPR3, SmOPR4, and  
433 SmOPR6) clustered together in subgroup VI. Because SmOPR1 showed OPR1 activity, the other  
434 OPRs in subgroup VI may be unrelated to JA biosynthesis. In contrast, the other known OPR3-  
435 like enzymes are positioned in the same cluster in subgroup II. It is most likely that OPR3-like  
436 enzymes independently evolved to expand the substrate binding pocket to accept *cis*-(+)-OPDA.

437

438 *SmJAR1*. JAR1 is responsible for conjugating JA to amino acids. Because JA-Ile is a versatile  
439 molecule in JA signaling, JAR1 is necessary for JA-mediated physiological events in seed plants  
440 (Wasternack and Hause 2013). JAR1 is a member of the GH3 proteins, which are classified into  
441 three groups based on their enzymatic activity. Group I proteins, such as *Arabidopsis* AtJAR1,  
442 can synthesize the JA-amino acid conjugates JA-Ile, JA-Leu and JA-Val (Staswick and Tiryaki  
443 2004). Group II proteins conjugate IAA and SA to various amino acids (Staswick et al. 2005).  
444 Group III proteins accept benzoates as substrates for amino acid conjugation (Okrent et al. 2009).  
445 A group I GH3 protein from seed plants showed JA-Ile synthase activity, which functions in  
446 defense (Kang et al. 2006, Wang et al. 2007, Suza et al. 2010).

447 *S. moellendorffii* produces JA-Ile based on evidence of a functionally active SmJAR1 (Fig. 7).  
448 The identification of JA-Ile and an active SmJAR1 strongly suggests that JA-Ile-mediated  
449 signaling is functional in *S. moellendorffii*. Moreover, SmJAR1 was hypothesized to prefer Ile as  
450 a substrate for conjugation with JA (Fig. 7 and Supplementary Fig. S16). The same characteristic  
451 was also found in AtJAR1 (Staswick and Tiryaki 2004, Suza and Staswick 2008). Considering

452 the substrate specificity of SmJAR1, JA-Ile seems to be more important than the other JA-amino  
453 acid conjugates. Additionally, endogenous conjugates of JA with another amino acid, such as JA-  
454 Trp, JA-Phe, JA-Gly, JA-Leu, and JA-Val, have not been found in *S. moellendorffii*  
455 (Supplementary Fig. 19).

456 In the case of rice (*Oryza sativa*), OsJAR2 in the cluster of group II GH3 proteins can  
457 conjugate JA to Ile, similar to OsJAR1 in the cluster of group I GH3 proteins (Wakuta et al.  
458 2011). The other thirteen of JAR1 homologs found in *S. moellendorffii* might also show JA-Ile  
459 synthetic activity. Given that GH3 proteins synthesize conjugates of JA and amino acids in *P.*  
460 *patens* (Ludwig-Müller et al. 2009), land plants are suggested to have enzymes with ubiquitous  
461 JAR1 activity. JA synthesis and JAR1 activity might have evolved independently in land plants.

462

463 *Expression of SmAOC1, SmOPR5, and SmJARI*

464 Wounding and JA induce the expression of various genes involved in defense responses in  
465 seed plants, i.e., genes encoding enzymes in JA biosynthesis. In *S. moellendorffii*, the expression  
466 of *SmAOC1* and *SmOPR5* under wounding treatment was increased, respectively (Fig. 8). These  
467 results were consistent with the transient increases in OPDA and JA in *S. moellendorffii* (Fig. 3).  
468 Based on the *SmOPR5* expression level, the accumulation of *SmOPR5* appears to precede the  
469 production of OPDA. Additionally, the late accumulation of JA-Ile coincided with the late  
470 expression level of *SmJARI* after wounding (Fig. 8). The expression profiles of *SmAOC1*,  
471 *SmOPR5*, and *SmJARI* support the accumulation patterns of OPDA, JA, and JA-Ile, probably due  
472 to the role of jasmonates in regulating responses to environmental stress in *S. moellendorffii*.

473 The present study also demonstrated that JA induced the expression of *SmAOC1* and  
474 *SmOPR5* in *S. moellendorffii*. JA treatment led to the accumulation of genes encoding enzymes in

475 the octadecanoid pathway, indicating positive feedback regulation of JA biosynthesis. The  
476 expression of *SmAOC1* and *SmOPR5* was enhanced upon JA application, and these expression  
477 patterns were similar to those observed under wounding treatment (Fig. 9). The JA-induced  
478 expression of *SmAOC1* and *SmOPR5* allows us to infer the presence of positive feedback  
479 regulation of JA biosynthesis in *S. moellendorffii*. In contrast to the up-regulation of *SmJAR1* by  
480 wounding, JA inhibited *SmJAR1* expression at the transcriptional level (Fig. 9). Although the  
481 detailed JA signaling pathway has not been elucidated in *S. moellendorffii*, the suppression of  
482 *SmJAR1* expression by JA appears to function as negative feedback regulation of JA-Ile-mediated  
483 signaling and/or an increase in JA signaling that is independent from JA-Ile. Wounding probably  
484 activates various signaling pathways that are JA-dependent and JA-independent. In the case of  
485 *SmJAR1* expression, integrated signaling caused by wounding might induce *SmJAR1* expression  
486 against stresses.

487

488 *OPDA, JA, and JA-Ile inhibit the growth of S. moellendorffii*

489 *P. patens* and *M. polymorpha* cannot produce JA; instead, OPDA inhibits their growth, and  
490 JA does not induce any significant physiological responses (Stumpe et al. 2010, Yamamoto et al.  
491 2015). However, *P. patens* responds to methyl jasmonate, which has not been detected in *P.*  
492 *patens*, by reducing its colony size (Ponce de León et al. 2012). Many studies have reported the  
493 growth inhibitory activity of JA in seed plants. OPDA, JA, and JA-Ile treatment retarded the  
494 growth of *S. moellendorffii* in a manner similar to those of seed plants (Fig. 10, Supplementary  
495 Fig. 18). This report is the first evidence that OPDA, JA and JA-Ile inhibit the growth of non-  
496 seed vascular plants. The growth inhibitory activity of JA and JA-Ile is probably a characteristic  
497 physiological response that is conserved in vascular plants. During plant evolution, JA

498 biosynthesis and signaling in vascular plants might have developed due to the need to adapt to  
499 life on land and/or to organize more complicated physiological processes.

500 It has recently been reported that the genes encoding proteins related to JA signaling  
501 perception, such as COI1 and JAZ, are present in bryophytes and lycophytes (Wang et al. 2015).  
502 The JA responsiveness of *S. moellendorffii* shown in this study indicates that JA might function  
503 through a signal transduction mechanism similar to that observed in seed plants: the COI1-JAZ  
504 system. Given that JA does not have any significant effect in bryophytes, vascular plants are  
505 suggested to have developed the COI1-JAZ system, which is suitable for JA signaling.  
506 Investigating the functional difference in the COI1-JAZ system between bryophytes and  
507 lycophytes is important for understanding the functional evolution of JA signal transduction in  
508 plants. *S. moellendorffii* will be a key plant for understanding the function of JA in vascular  
509 plants.

510 In conclusion, we provide the first evidence of the presence of OPDA, JA, and JA-Ile in the  
511 model lycophyte *S. moellendorffii*, which is taxonomically positioned between bryophytes and  
512 euphylllophytes. Moreover, active homologous enzymes involved in the octadecanoid pathway,  
513 including an AOS, an AOC, an OPR3-like enzyme, and a JAR1, were also identified in this plant.  
514 The application of exogenous OPDA, JA, and JA-Ile significantly inhibited the growth of *S.*  
515 *moellendorffii*. Thus, OPDA, JA, and JA-Ile are probably important signaling molecules in stress  
516 responses and growth regulators in *S. moellendorffii*.

517

## 518 **Materials and Methods**

519 *Plant material*

520        *S. moellendorffii* was grown at 25°C under white fluorescent light with a photoperiod of 14 h  
521        light/10 h dark.

522  
523        *Analysis of OPDA, JA, and JA-Ile*  
524        The microphylls and stems of *S. moellendorffii* (ca. 500 mg) were harvested 10, 20, 30, 60 or  
525        180 min after wounding with tweezers and were homogenized in liquid nitrogen, followed by  
526        ethanol extraction for 24 h. UPLC-MS/MS analysis was performed according to Sato et al.  
527        (2009) and Yamamoto et al. (2015).

528  
529        *JA growth inhibitory activity assay in S. moellendorffii*  
530        *S. moellendorffii* bulbils (Supplementary Fig. S17) were sprinkled onto a Jiffy-7 pellet  
531        (Sakata Seed Corporation, Japan). The bulbils were grown at 25°C under white fluorescent light  
532        with a photoperiod of 14 h light/10 h dark. After germination and one week of growth, the plants  
533        were treated with OPDA, JA, or JA-Ile at concentrations of 25 µM, 50 µM, and 100 µM every  
534        other day for four weeks. The shoot growth of the plants was evaluated by morphometric analysis.

535  
536        *Bioinformatics analysis*  
537        All of the putative genes in *S. moellendorffii* were screened in the Phytozome v 11.0 database  
538        (<https://phytozome.jgi.doe.gov/pz/portal.html>) using the *Arabidopsis* amino acid sequence as a  
539        query (Supplementary Table S1). Multiple sequence analysis was performed using Clustal  
540        Omega and viewed in the GeneDoc software program. A phylogenetic tree was generated using  
541        Mega version 5.2 (Neighbor-joining method). Bootstrap analysis was performed by resampling  
542        the datasets 1,000 times. The sub-cellular localization of *SmAOC1* was predicted using ChloroP v

543 1.1 (<http://www.cbs.dtu.dk/services/ChloroP/>) and TargetP (<http://www.cbs.dtu.dk/services/TargetP/>). The theoretical pI and molecular weight were analyzed using the Compute pI/Mw tool  
544 ([http://web.expasy.org/compute\\_pi/](http://web.expasy.org/compute_pi/)).

546

547 *Molecular cloning of SmAOS2, SmAOC1, SmOPR1, SmOPR5, and SmJAR1-I*

548 The *SmAOS2*, *SmAOC1*, *SmOPR1*, *SmOPR5*, and *SmJAR1* genes were cloned according to a  
549 conventional method. The details are described in the Supplemental Information.

550

551 *Synthesis of recombinant SmAOS2, SmAOC1, SmOPR1 and SmOPR5*

552 Recombinant SmAOS2, SmAOC1, SmOPR1 and SmOPR5 were produced according to a  
553 conventional method. The details are described in the Supplemental Information.

554

555 *Enzyme assay of SmAOS2*

556 To measure AOS activity, SmAOS2 was reacted with 13(*S*)-HPOT according to Bandara et al.  
557 (2009) with some modifications. Five milligrams of recombinant SmAOS2 was reacted with 6 µg  
558 of 13(*S*)-HPOT as a substrate in a total volume of 0.1 ml of 50 mM phosphate buffer (pH 7.0).  
559 The reaction mixture was incubated at 25°C for 1 h. To terminate the enzymatic reaction, the  
560 mixture was treated with 1 M HCl until it reached pH 3. To convert *cis*-OPDA to *trans*-OPDA,  
561 the reaction mixture was subjected to alkaline treatment by stirring with 1 ml of 1 M NaOH for  
562 30 min. After acidification, the resulting solution was extracted three times with an identical  
563 volume of ethyl acetate, evaporated, and methylated using ethereal diazomethane. After  
564 incubation for 30 min on ice, the reaction was terminated with the addition of 1 or 2 drops of  
565 acetic acid until the color changed from yellow to colorless. The methylated residue was

566 dissolved in 100  $\mu$ l of CHCl<sub>3</sub> for chiral GC-MS analysis (1200 L GC-MS/MS system, Varian,  
567 USA) equipped with a  $\beta$ -DEX fused silica capillary column (0.25 mm  $\times$  30 m  $\times$  0.25  $\mu$ m,  
568 Supelco, USA). Helium was used as the carrier gas at a constant flow rate of 1.0 ml/min. The ion  
569 source and vaporizing chamber were heated to 200°C and 220°C, respectively, and the ionization  
570 voltage was 70 eV. The column was initially heated to 50°C and held isothermally for 1 min, and  
571 then the temperature was subsequently increased at a rate of 10°C/min to a final temperature of  
572 190°C, which was held for 80 min.

573

574 *Enzyme assay of SmAOC1 activity*

575 The enzymatic reaction was performed in a mixture of 5  $\mu$ g of 13-HPOT and 5  $\mu$ g of  
576 PpAOS1 in 1 ml of 10 mM sodium phosphate buffer (pH 7.8) with or without 10  $\mu$ g of SmAOC1.  
577 The reaction mixture was incubated at 25°C for 1 h. The products of the SmAOC1 reaction were  
578 analyzed according to the method of OPDA analysis described in the previous section.

579

580 *Enzyme assays for OPR activity*

581 The enzymatic reaction was performed according to the method of Schaller et al. (1998) with  
582 some modifications. Five micrograms of affinity-purified recombinant SmOPR1 or SmOPR5 was  
583 incubated in 50 mM potassium phosphate buffer (pH 7.4) containing 7.5  $\mu$ g of ( $\pm$ )-*cis*-OPDA as a  
584 substrate and 1.0 mM NADPH in a total volume of 0.1 ml for 1 h at 25°C. At the end of the  
585 incubation, ( $\pm$ )-*cis*-OPDA and ( $\pm$ )-*cis*-OPC-8:0 were converted to methylated *trans*-isomers  
586 according to the method described above. OPC-8:0 was evaluated by chiral GC-MS analysis  
587 (same conditions as the enzymatic analysis for SmAOC1).

588

589 *Subcellular localization of SmAOC1*

590 Subcellular localization of SmAOC1 was analyzed according to the method of Yamamoto et  
591 al. (2015). The details are described in the Supplemental Information.

592

593 *Enzyme assays for JAR1 activity*

594 SmJAR1 activity was assayed according to Wakuta et al. (2011) with some modifications. *E.*  
595 *coli* BL21 (DE3) cells carrying pET23a-SmJAR1 were cultured overnight in 5 ml of LB medium  
596 supplemented with 100 µg/ml ampicillin, at 37°C. A portion of the culture was inoculated into 2  
597 ml of fresh selective LB medium, incubated until the OD<sub>600</sub> reached 0.2, and treated with 1 mM  
598 IPTG. The culture was incubated at 37°C for 5 h to induce protein production. Subsequently, 0.2  
599 mM JA was added to the culture. The incubation was continued at 37°C for 3 h with shaking. JA-  
600 Ile in the culture was analyzed using the UPLC-MS/MS system as previously described (Sato et  
601 al. 2009).

602

603 *Quantitative RT-PCR for SmAOC1, SmOPR5, and SmJAR in S. moellendorffii exposed to*  
604 *wounding stress and JA treatments*

605 The coding sequences (CDSs) for *SmAOC1*, *SmOPR5*, and *SmJAR1* were used to design  
606 specific primers for quantitative RT-PCR (qRT-PCR). The primers used to amplify these genes  
607 are listed in Supplementary Table S1. Total RNA of *S. moellendorffii* was extracted 0, 10, 20, 30,  
608 60, and 180 min after wounding or 50 µM JA treatment. The first-strand cDNA was used as a  
609 template. In the present study, KOD SYBR qPCR Mix (Toyobo, Japan) was used according to  
610 the manufacturer's protocol. Each reaction mixture contained 12.5 µl of KOD SYBR® qPCR Mix,  
611 1 µl of each primer (10 mM), 1 µl of cDNA, and 9.5 µl of MilliQ water qRT-PCR was performed

612 on a Thermal Cycler Dice Real Time system (Takara TP800, Japan). The qRT-PCR conditions  
613 were as follows: pre-incubation at 95°C for 30 s, followed by 40 cycles of 95°C for 5 s and 60°C  
614 for 30 s. The specificity of each PCR amplicon was assessed with a dissociation curve (95°C for  
615 15 s, 60°C for 30 s, and 95°C at 15 s). Each target gene was calculated and expressed as fold  
616 regulation in comparison to the housekeeping genes actin (XM\_002976966) for the wounding  
617 treatment and ubiquitin EST (DN839032, Kirkbride et al. 2013) for the JA treatment.

618

619 **Funding information**

620 This research was supported by grants from Hokkaido University.

621

622 **Disclosures**

623 The authors have no conflicts of interest to declare.

624

625 **Acknowledgements**

626 The authors are grateful to Dr. Hasabe at the National Institute for Basic Biology for kindly  
627 providing *S. moellendorffii* and the plasmid, pUGWnew5. Methyl jasmonate, which was needed  
628 to synthesize deuterium-labeled compounds, was kindly provided by Zeon corporation (Tokyo,  
629 Japan).

630

631    **References**

- 632    Agrawal, G., Jwa, N.S., Agrawal, S.K., Tamogami, S., Iwahashi, H. and Rakwal, R. (2003)  
633    Cloning of novel rice allene oxide cyclase (*OsAOC*): mRNA expression and comparative analysis  
634    with allene oxide synthase (*OsAOS*) gene provides insight into the transcriptional regulation of  
635    octadecanoid pathway biosynthetic genes in rice. *Plant Sci.* 164: 979-992.  
636  
637    Banks, J.A. (2009) *Selaginella* and 400 million years of separation. *Annu. Rev. Plant Biol.* 60:  
638    223-238.  
639  
640    Banks, J.A., Nishiyama, T., Hasebe, M., Bowman, J.L., Grabskov, M., dePamphilis, C., et al.  
641    (2011) The *Selaginella* genome identifies genetic changes associated with the evolution of  
642    vascular plants. *Science* 332: 960-963.  
643  
644    Breithaupt, C., Kurzbauer, R., Schaller, F., Stintzi, A., Schaller, A., Huber, R., et al. (2009)  
645    Structural basis of substrate specificity of plant 12-oxophytodienoate reductases. *J. Mol. Biol.*  
646    392: 1266-1277.  
647  
648    Chang, K.H., Xiang, H. and Dunaway-Mariano, D. (1997) Acyl-adenylate motif of the acyl-  
649    adenylate/thioester-forming enzyme superfamily: a site-directed mutagenesis study with the  
650    *Pseudomonas* sp. strain CBS3 4-chlorobenzoate:coenzyme A ligase. *Biochemistry* 36: 15650–  
651    15659.  
652

- 653 Conconi, A., Miquel, M., Browse, J.A. and Ryan, C.A. (1996) Intracellular levels of free  
654 linolenic and linoleic acids increase in tomato leaves in response to wounding. *Plant Physiol.*  
655 111: 797-803.
- 656
- 657 Creelman, R.A. and Mullet, J.E. (1997) Biosynthesis and action of jasmonates in plants. *Annu.*  
658 *Rev. Plant Physiol. Mol. Biol.* 48: 355-381.
- 659
- 660 Farmaki, T., Sanmartín, M., Jiménez, P., Paneque, M., Sanz, C., Vancanneyt, G., et al. (2007)  
661 Differential distribution of the lipoxygenase pathway enzymes within potato chloroplasts. *J. Exp.*  
662 *Bot.* 58: 555-568.
- 663
- 664 Farmer, E.E. and Ryan, C.A. (1992) Octadecanoid precursors of jasmonic acid activate the  
665 synthesis of wound-inducible proteinase inhibitors. *Plant Cell* 4: 129-134.
- 666
- 667 Fonseca, S., Chico, J.M. and Solano, R. (2009a) The jasmonate pathway: the ligand, the receptor  
668 and the core signalling module. *Curr. Opin. Plant Biol.* 12: 539-547.
- 669
- 670 Fonseca, S., Chini, A., Hamberg, M., Adie, B., Porzel, A., Kramell, R., et al. (2009b) (+)-7-*iso-*  
671 Jasmonyl-L-isoleucine is the endogenous bioactive jasmonate. *Nat. Chem. Biol.* 5: 344-350.
- 672
- 673 Hashimoto, T., Takahashi, K., Sato, M., Bandara, P.K.G.S.S. and Nabeta, K. (2011) Cloning and  
674 characterization of an allene oxide cyclase, PpAOC3, in *Physcomitrella patens*. *Plant Growth*  
675 *Regul.* 65: 239-245.

- 676
- 677 Hecht, J., Grewe, F. and Knoop, V. (2011) Extreme RNA editing in coding islands and abundant  
678 microsatellites in repeat sequences of *Selaginella moellendorffii* mitochondria: the root of  
679 frequent plant mtDNA recombination in early tracheophytes. *Genome Biol. Evol.* 3: 344-358.
- 680
- 681 Hyun, Y., Choi, S., Hwang, H.J., Yu, J., Nam, S.J., Ko, J., et al. (2008) Cooperation and  
682 functional diversification of two closely related galactolipase genes for jasmonate biosynthesis.  
683 *Dev. Cell* 14: 183-192.
- 684
- 685 Ishiguro, S., Kawai-Oda, A., Ueda, J., Nishida, I. and Okada, K. (2001) The DEFECTIVE IN  
686 ANOTHER DEHISCENCE gene encodes a novel phospholipase A1 catalyzing the initial step of  
687 jasmonic acid biosynthesis, which synchronizes pollen maturation, anther dehiscence, and flower  
688 opening in *Arabidopsis*. *Plant Cell* 13: 2191-2209.
- 689
- 690 Kang, J.H., Wang, L., Giri, A. and Baldwin, I.T. (2006) Silencing threonine deaminase and JAR4  
691 in *Nicotiana attenuata* impairs jasmonic acid-isoleucine-mediated defenses against *Manduca*  
692 *sexta*. *Plant Cell* 18: 3303–3320.
- 693
- 694 Kenrick, P. and Crane, P.R. (1997) The origin and early evolution of plants on land. *Nature* 389:  
695 33-39.
- 696
- 697 Khan, M.I.R., Syeed, S., Nazar, R. and Anjum, N.A. (2012) An insight into the role of salicylic  
698 acid and jasmonic acid in salt stress tolerance. In *Phytohormones and Abiotic Stress Tolerance in*

699 *Plants*. Edited by Khan, N.A., Nazar, R., Iqbal, N. and Anjum, N.A. pp. 277-300. Springer  
700 Verlag, New York.

701  
702 Kirkbirdie, R.C., Fischer, R.L., Harada, J.J. (2013) Leafy cotyledon1, a key regulator of seed  
703 development, is expressed in vegetative and sexual propagules of *Selaginella moellendorffii*.  
704 *PLOS ONE* 8: e67971. doi:10.1371/journal.pone.0067971.

705  
706 Kitaoka, N., Matsubara, T., Sato, M., Takahashi, K., Wakuta, S., Kawaide, H., et al. (2011)  
707 *Arabidopsis* CYP94B3 encodes jasmonyl-L-isoleucine 12-hydroxylase, a key enzyme in the  
708 oxidative catabolism of jasmonate. *Plant Cell Physiol.* 52: 1757-1765.

709  
710 Koeduka, T., Ishizaki, K., Mwenda, C.M., Hori, K., Sasaki-Sekimoto, Y., Ohta, H., et al. (2015)  
711 Biochemical characterization of allene oxide synthases from the liverwort *Marchantia*  
712 *polymorpha* and green microalgae *Klebsormidium flaccidum* provides insight into the  
713 evolutionary divergence of the plant CYP74 family. *Planta* 242:1175-1786.

714  
715 Koo, A.J., Cooke, T.F. and Howe, G.A. (2011) Cytochrome P450 CYP94B3 mediates catabolism  
716 and inactivation of the plant hormone jasmonoyl-L-isoleucine. *Proc. Natl Acad. Sci. USA.* 108:  
717 9298-9303.

718  
719 Laudert, D., Hennig, P., Stelmach, B.A., Müller, A., Andert, L. and Weiler, E.W. (1997) Analysis  
720 of 12-oxo-phytodienoic acid enantiomers in biological samples by capillary gas chromatography-  
721 mass spectrometry using cyclodextrin stationary phases. *Anal. Biochem.* 246: 211-217.

- 722
- 723 Li, W., Liu, B., Yu, L., Feng, D., Wang, H. and Wang, J. (2009) Phylogenetic analysis, structural  
724 evolution and functional divergence of the 12-oxo-phytodienoate acid reductase gene family in  
725 plants. *BMC Evol. Biol.* 9: 90.
- 726
- 727 Ludwig-Müller, J., Jülke, S., Bierfreund, N.M., Decker, E.L. and Reski, R. (2009) Moss  
728 (*Physcomitrella patens*) GH3 proteins act in auxin homeostasis. *New Phytol.* 181: 323-338.
- 729
- 730 Maucher, H., Stenzel, I., Miersch, O., Stein, N., Prasad, M., Zierold, U., et al. (2004) The allene  
731 oxide cyclase of barley (*Hordeum vulgare* L.)--cloning and organ-specific expression.  
732 *Phytochemistry* 65: 801-811.
- 733
- 734 Mueller, M.J., Brodschelm, W., Spannagl, E. and Zenk, M.H. (1993) Signaling in the elicitation  
735 process is mediated through the octadecanoid pathway leading to jasmonic acid. *Proc. Natl Acad.*  
736 *Sci. USA* 90: 7490-7494.
- 737
- 738 Narváez-Vásquez, J., Florin-Christensen, J. and Ryan, C.A. (1999) Positional specificity of a  
739 phospholipase A activity induced by wounding, systemin, and oligosaccharide elicitors in tomato  
740 leaves. *Plant Cell* 11: 2249-2260.
- 741
- 742 Okrent, R.A., Brooks, M.D. and Wildermuth, M.C. (2009) *Arabidopsis* GH3.12 (PBS3)  
743 conjugates amino acids to 4-substituted benzoates and is inhibited by salicylate. *J. Biol. Chem.*  
744 284: 9742-9754.

- 745
- 746 Penninckx, I.A., Eggermont, K., Terras, F.R., Thomma, B.P., de Samblanx, G.W., Buchala, A., et  
747 al. (1996) Pathogen-induced systemic activation of a plant defensin gene in *Arabidopsis* follows a  
748 salicylic acid-independent pathway. *Plant Cell* 8: 2309-2323.
- 749
- 750 Pi, Y., Liao, Z., Jiang, K., Huang, B., Deng, Z., Zhao, D., et al. (2008) Molecular cloning,  
751 characterization and expression of a jasmonate biosynthetic pathway gene encoding allene oxide  
752 cyclase from *Camptotheca acuminata*. *Biosci. Rep.* 28: 349-355.
- 753
- 754 Ponce de León, I., Schmelz, E.A., Gaggero, C., Castro, A., Álvarez, A. and Montesano, M.  
755 (2012) *Physcomitrella patens* activates reinforcement of the cell wall, programmed cell death and  
756 accumulation of evolutionary conserved defence signals, such as salicylic acid and 12-oxo-  
757 phytodienoic acid, but not jasmonic acid, upon *Botrytis cinerea* infection. *Mol. Plant. Pathol.*.. 13:  
758 960-974.
- 759
- 760 Radhika, V., Kost, C., Bonaventure, G., David, A. and Boland, W. (2012) Volatile emission in  
761 bracken fern is induced by jasmonates but not by *Spodoptera littoralis* or *Strongylogaster*  
762 *multifasciata* herbivory. *PLOS ONE* 7: e48050.
- 763
- 764 Santino, A., Taurino, M., De Domenico, S., Bonsegna, S., Poltronieri, P., Pastor, V., et al. (2013)  
765 Jasmonate signaling in plant development and defense response to multiple (a)biotic stresses.  
766 *Plant Cell Rep.* 32: 1085-1098.
- 767

768 Sato, C., Seto, Y., Nabetu, K. and Matsuura, H. (2009) Kinetics of the accumulation of jasmonic  
769 acid and its derivatives in systemic leaves of tobacco (*Nicotiana tabacum* cv. *Xanthi nc*) and  
770 translocation of deuterium-labeled jasmonic acid from the wounding site to the systemic site.  
771 *Biosci. Biotechnol. Biochem.* 73: 1962-1970.

772

773 Schaller, F., Hennig, P. and Weiler, E.W. (1998) 12-Oxophytodienoate-10,11-reductase:  
774 occurrence of two isoenzymes of different specificity against stereoisomers of 12-  
775 oxophytodienoic acid. *Plant Physiol* 118: 1345-1351.

776

777 Schaller, A. and Stintzi A. (2009) Enzymes in jasmonate biosynthesis - structure, function,  
778 regulation. *Phytochemistry* 70:1532-1538.

779

780 Sheard, L.B., Tan, X., Mao, H., Withers, J., Ben-Nissan, G., Hinds, T.R., et al. (2010) Jasmonate  
781 perception by inositol-phosphate-potential COI1-JAZ co-receptor. *Nature* 468: 400-405.

782

783 Staswick, P.E., Serban, B., Rowe, M., Tiryaki, I., Maldonado, M.T., Maldonado, M.C., et al.  
784 (2005) Characterization of an *Arabidopsis* enzyme family that conjugates amino acids to indole-  
785 3-acetic acid. *Plant Cell* 17: 616-627.

786

787 Staswick, P.E. and Tiryaki, I. (2004) The oxylipin signal jasmonic acid is activated by an enzyme  
788 that conjugates it to isoleucine in *Arabidopsis*. *Plant Cell* 16: 2117-2127.

789

- 790 Stenzel, I., Hause, B., Miersch, O., Kurz, T., Maucher, H., Weichert, H., et al. (2003) Jasmonate  
791 biosynthesis and the allene oxide cyclase family of *Arabidopsis thaliana*. *Plant Mol. Biol.* 51:  
792 895-911.
- 793
- 794 Stenzel, I., Otto, M., Delker, C., Kirmse, N., Schmidt, D., Miersch, O., et al. (2012) Allene oxide  
795 cyclase (AOC) gene family members of *Arabidopsis thaliana*: tissue- and organ- specific  
796 promoter activities and in vivo heteromerization. *J. Exp. Bot.* 63: 6125-6138.
- 797
- 798 Stumpe, M., Göbel, C., Faltin, B., Beike, A.K., Hause, B., Himmelsbach, K., et al. (2010) The  
799 moss *Physcomitrella patens* contains cyclopentenones but no jasmonates: mutations in allene  
800 oxide cyclase lead to reduced fertility and altered sporophyte morphology. *New Phytol.* 188: 740-  
801 749.
- 802
- 803 Suza, W.P., Rowe, M.L., Hamberg, M. and Staswick, P.E. (2010) A tomato enzyme synthesizes  
804 (+)-7-*iso*-jasmonoyl-L-isoleucine in wounded leaves. *Planta* 231: 717-728.
- 805
- 806 Suza, W.P. and Staswick, P.E. (2008) The role of JAR1 in Jasmonoyl-L-isoleucine production  
807 during *Arabidopsis* wound response. *Planta* 227: 1221-1232.
- 808
- 809 Vick, B.A. and Zimmerman, D.C. (1983) The biosynthesis of jasmonic acid: a physiological role  
810 for plant lipoxygenase. *Biochem. Biophys. Res. Commun.* 111: 470-477.
- 811

812 Wakuta, S., Suzuki, E., Saburi, W., Matsuura, H., Nabeto, K., Imai, R., et al. (2011) OsJAR1 and  
813 OsJAR2 are jasmonyl-L-isoleucine synthases involved in wound- and pathogen-induced  
814 jasmonic acid signalling. *Biochem. Biophys. Res. Commun.* 409: 634-639.

815

816 Wang, C., Liu, Y., Li, S.S. and Han, G.Z. (2015) Insights into the origin and evolution of the  
817 plant hormone signaling machinery. *Plant Physiol.* 167: 872-886.

818

819 Wang, L., Allmann, S., Wu, J. and Baldwin, I.T. (2008) Comparisons of LIPOXYGENASE3-  
820 and JASMONATE-RESISTANT4/6-silenced plants reveal that jasmonic acid and jasmonic acid-  
821 amino acid conjugates play different roles in herbivore resistance of *Nicotiana attenuata*. *Plant*  
822 *Physiol.* 146: 904–915.

823

824 Wasternack, C. (2007) Jasmonates: an update on biosynthesis, signal transduction and action in  
825 plant stress response, growth and development. *Ann. Bot.* 100: 681-697.

826

827 Wasternack, C. and Hause, B. (2013) Jasmonates: biosynthesis, perception, signal transduction  
828 and action in plant stress response, growth and development. An update to the 2007 review in  
829 *Annals of Botany*. *Ann. Bot.* 111: 1021-1058.

830

831 Wasternack, C. and Parthier, B. (1997) Jasmonate-signalled plant gene expression. *Trends Plant*  
832 *Sci.* 2: 302-307.

833

834 Weng, J.K., Tanurdzic, M. and Chapple, C. (2005) Functional analysis and comparative  
835 genomics of expressed sequence tags from the lycophyte *Selaginella moellendorffii*. *BMC*  
836 *Genomics* 6: 85.

837

838 Yamamoto, Y., Ohshika, J., Takahashi, T., Ishizaki, K., Kohchi, T., Matsuura, H., et al. (2015)  
839 Functional analysis of allene oxide cyclase, MpAOC, in the liverwort *Marchantia polymorpha*.  
840 *Phytochemistry* 116: 48-56.

841

842 Yan, Y., Borrego, E. and Kolomiets, M.V. (2013) Jasmonate biosynthesis, perception and  
843 function in plant development and stress responses. In *Lipid Metabolism*. Edited by Baez, R.V.  
844 pp. 393-442. Intech. DOI: 10.5772/52675.

845

846 Ziegler, J., Stenzel, I., Hause, B., Maucher, H., Hamberg, M., Grimm, R., et al. (2000) Molecular  
847 cloning of allene oxide cyclase. The enzyme establishing the stereochemistry of octadecanoids  
848 and jasmonates. *J. Biol. Chem.* 275: 19132-19138.

849

850

851

852

853

854

855

856

857 Table 1. Properties of *SmAOC1*, *SmOPR1*, *SmOPR5*, and *SmJAR1*.

Gene name	ORF length (bp)	Protein length (aa)	MW (Da)	Theoretical pI
<i>SmAOS1</i>	1458	485	54,107	6.01
<i>SmAOS2</i>	1404	467	52,079	6.35
<i>SmAOS3</i>	1458	485	54,071	5.89
<i>SmAOC1</i>	738	245	26,364	9.15
<i>SmOPR1*</i>	1131	376	41,588	6.28
<i>SmOPR5*</i>	1209	402	44,046	6.05
<i>SmJAR1</i>	1749	582	64,751	5.83

858 \* The numbering of *SmOPRs* was previously described by Li et al. (2009).

859

860

861

862

863

864

865      **Figure legends**

866

867      Fig. 1. The biosynthesis of JA and JA-Ile.

868

869      Fig. 2. UPLC-MS/MS analysis of OPDA, JA, and JA-Ile in *S. moellendorffii*. (A–C) MRM mode  
870      analysis of a specific daughter peak at *m/z* 164.99 that was derived from the peak at *m/z* 291.37  
871      [M–H]<sup>–</sup>. (D–F) MRM mode analysis of a specific daughter peak at *m/z* 58.71 that was derived  
872      from the peak at *m/z* 209.09 [M–H]<sup>–</sup>. (G–I) MRM mode analysis of a specific daughter peak at  
873      *m/z* 129.68 that was derived from the peak at *m/z* 322.03 [M–H]<sup>–</sup>. (A, D, G) Standard. (B, E, H) *S.*  
874      *moellendorffii* extract. (C, F, I) Co-injection of the standard and *S. moellendorffii* extract.

875

876      Fig. 3. Accumulation of OPDA, JA, and OPDA in *S. moellendorffii* after wounding. *S.*  
877      *moellendorffii* was subjected to mechanical wounding and then collected at the indicated time  
878      after wounding. The concentrations of OPDA, JA, and JA-Ile were analyzed by UPLC-MS/MS.  
879      The data are presented as the mean ± SD (*n* = 3). The asterisks represent a significant difference  
880      between the treated and control plants (Student's t-test, \**p* < 0.05, \*\**p* < 0.01).

881

882      Fig. 4. Chiral GC-MS analysis of the OPDA methyl ester. Recombinant SmAOS2 was reacted  
883      with the substrate 13(S)-HPOT, directly treated with alkaline solution and then methylated by  
884      ethereal diazomethane. The methylated OPDA was analyzed by GC-MS using a chiral capillary  
885      column. The data are presented as the total ion current chromatogram. The former and latter  
886      peaks represent the *trans*-(+)- and (-)-OPDA methyl esters, respectively (Laudert et al. 1997).

887

888 Fig. 5. Chiral GC-MS analysis of the OPDA methyl ester. Recombinant SmAOC1 was reacted  
889 with the substrate 13-HPOT and an allene oxide synthase (PpAOS1), directly treated with  
890 alkaline solution and then methylated by ethereal diazomethane. The methylated OPDA was  
891 analyzed by GC-MS using a chiral capillary column. The molecular ion peak of the OPDA  
892 methyl ester at  $m/z$  306 was monitored. The former and latter peaks represent the *trans*-(+)- and  
893 (-)-OPDA methyl ester, respectively (Laudert et al. 1997). (A) Racemic OPDA standard. (B)  
894 Product of the SmAOC1 enzymatic reaction.

895

896 Fig. 6. Chiral GC-MS analysis of the reaction products catalyzed by SmOPR1 and SmOPR5.  
897 Recombinant SmOPR1 and SmOPR5 were each reacted with racemic OPDA, directly treated  
898 with alkaline solution and then methylated by ethereal diazomethane. The methylated reaction  
899 products were analyzed by GC-MS using a chiral capillary column. The data are presented as the  
900 total ion current chromatogram. Peaks 1 to 4 represent *trans*-isomers of (+)-OPC-8:0 (natural  
901 type), (-)-OPC-8:0, (+)-OPDA (natural type) and (-)-OPDA, respectively, that were derived  
902 from *cis*-isomers of these compounds.

903

904 Fig. 7. UPLC-MS/MS analysis of JA-Ile in *E. coli* overexpressing SmJAR1. MRM mode analysis  
905 of a specific daughter peak of JA-Ile- $d_6$  at  $m/z$  129.68 that was derived from the peak at  $m/z$   
906 328.03 [M-H] $^-$  and of the peak at  $m/z$  129.68 that was derived from the peak of JA-Ile at  $m/z$   
907 322.03 [M-H] $^-$ . (A) Internal standard JA-Ile- $d_6$ . (B) Culture supernatant of *E. coli*  
908 overexpressing SmJAR1. (C) Culture supernatant of *E. coli* containing pET23a as a control. \*The  
909 value of 100% is equal to  $9 \times 10^5$  counts, which was converted by the algorithm in Mass Lynx  
910 software (Waters Corporation, Milford, MA, USA).

911  
912 Fig. 8. Quantitative RT-PCR analysis of *SmAOC1*, *SmOPR5*, and *SmJAR1* in wounded *S.*  
913 *moellendorffii*. Plants were subjected to mechanical wounding and then collected at the indicated  
914 times after wounding. To evaluate the transcript levels of *SmAOC1*, *SmOPR5*, and *SmJAR1*,  
915 qRT-PCR was performed using RNA isolated from control and wounded plants. The data are  
916 presented as the mean ± SD (n = 3). The asterisks represent a significant difference between the  
917 treated and control plants (Student's t-test, \*p < 0.05; \*\*p < 0.01).

918  
919 Fig. 9. Quantitative RT-PCR analysis of *SmAOC1*, *SmOPR5*, and *SmJAR1* in *S. moellendorffii*  
920 treated with JA. Plants were treated with 50 µM JA and then collected at the indicated times after  
921 JA treatment. To evaluate the transcript levels of *SmAOC1*, *SmOPR5*, and *SmJAR1*, qRT-PCR  
922 was performed using RNA isolated from control and JA-treated plants. The data are presented as  
923 the mean ± SD (n = 3). The asterisks represent a significant difference between the treated and  
924 control plants (Student's t-test, \*p < 0.05; \*\*p < 0.01; \*\*\*p < 0.001).

925  
926 Fig. 10. Growth inhibitory activities of OPDA, JA, and JA-Ile in *S. moellendorffii*. *S.*  
927 *moellendorffii* was treated with OPDA, JA, and JA-Ile for four weeks, and then the shoots were  
928 measured. The data are presented as the mean ± SD (n = 5). The asterisks represent a significant  
929 difference between the treated and control plants (Student's t-test, \*\*p < 0.01; \*\*\*p < 0.001).

930  
931  
932

Fig. 1.

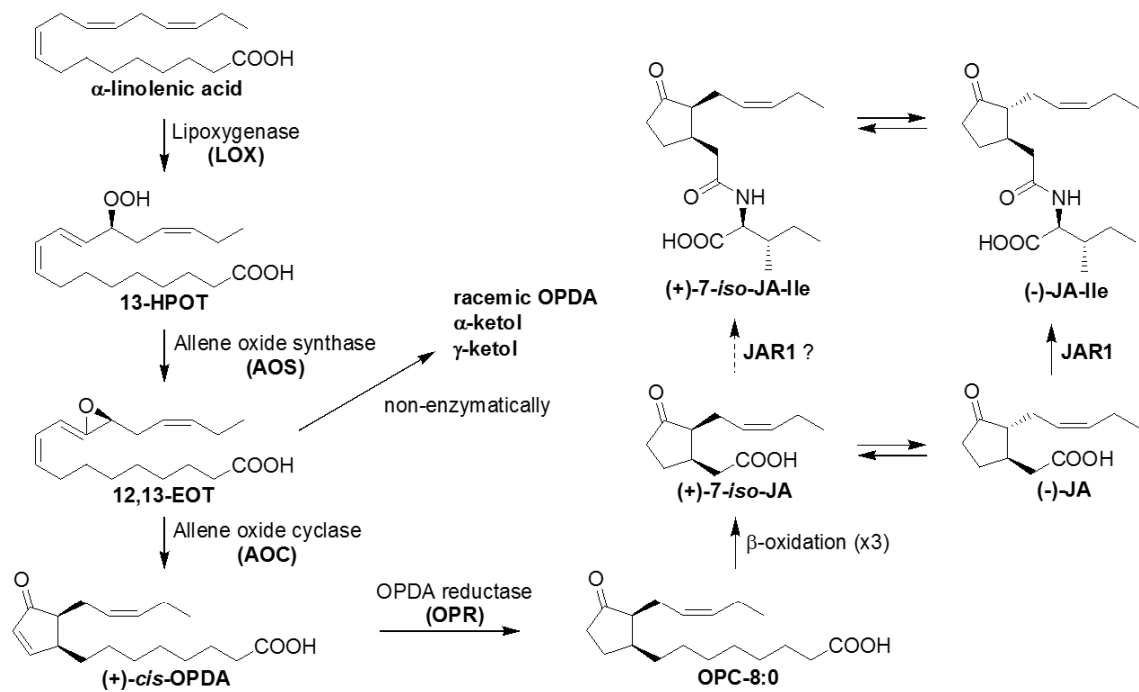


Fig. 2.

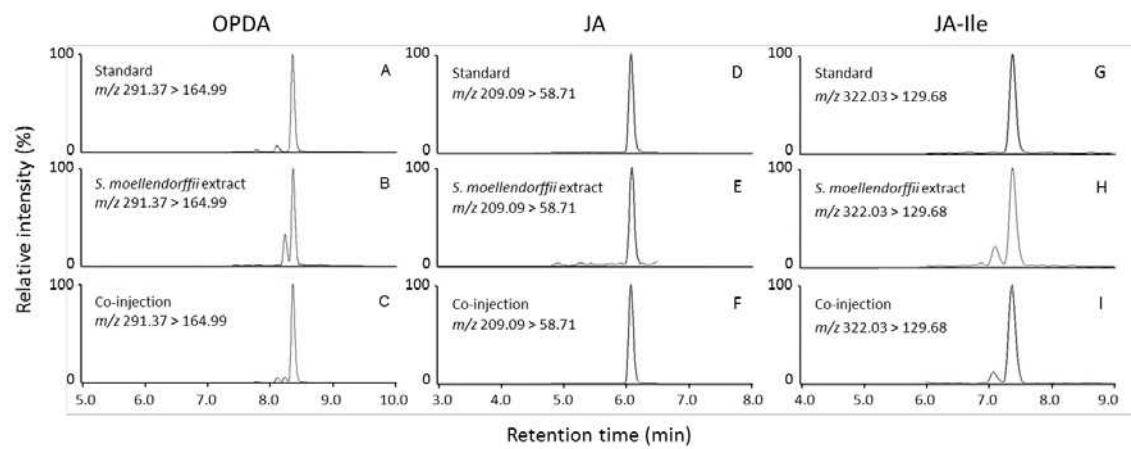


Fig. 3.

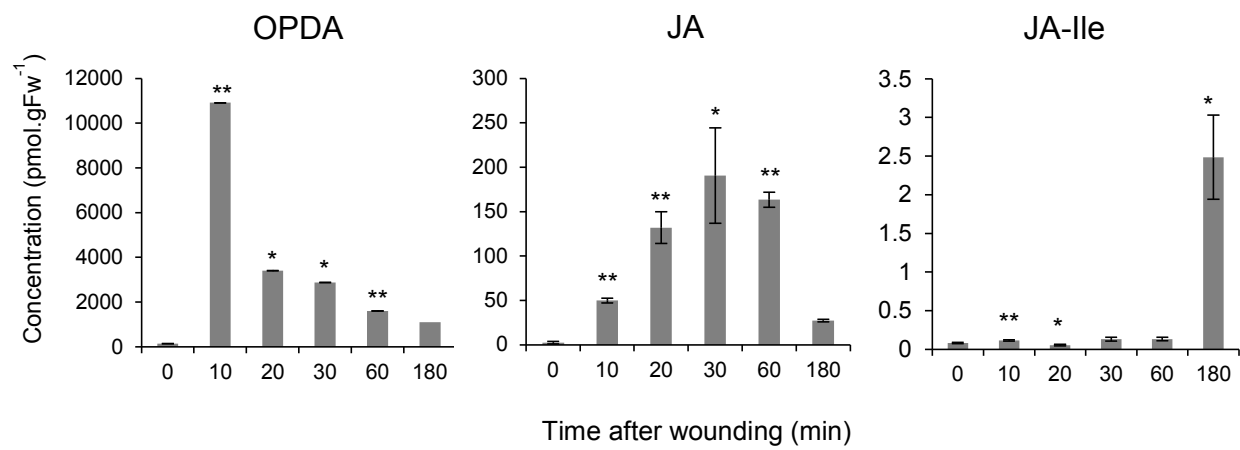


Fig. 4.

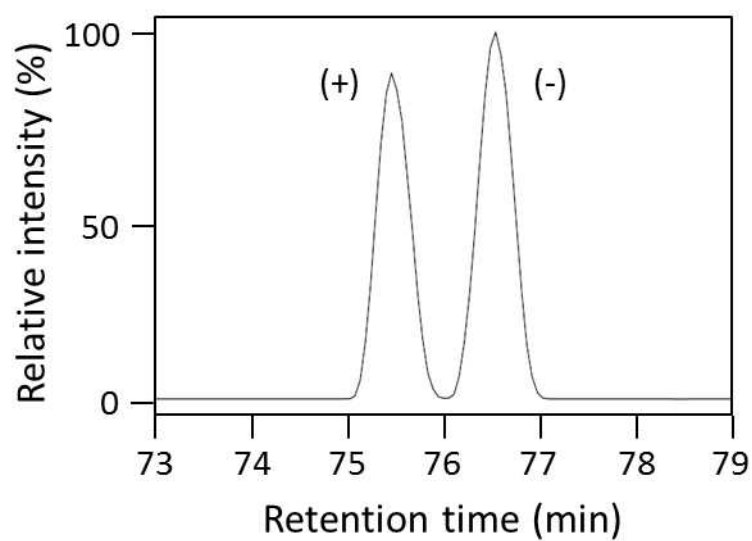


Fig. 5.

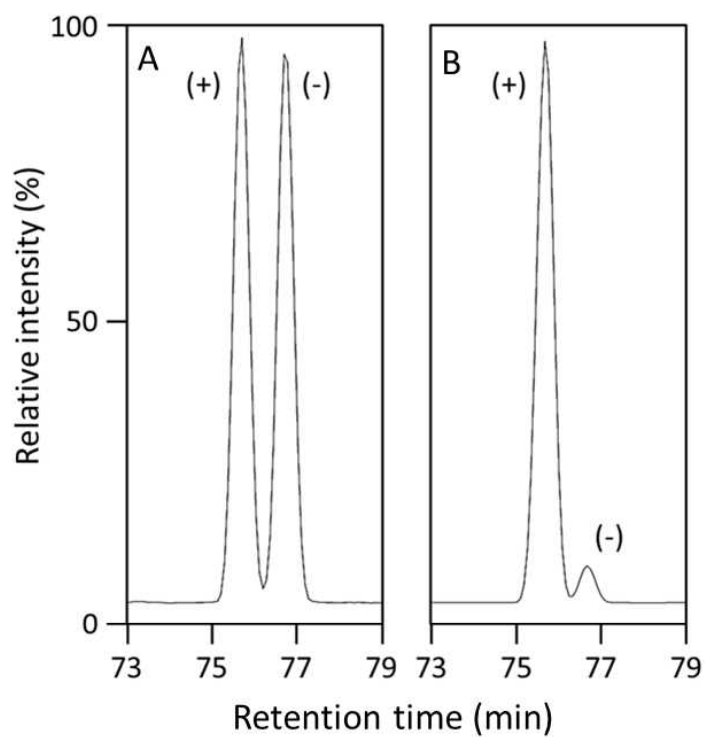


Fig. 6.

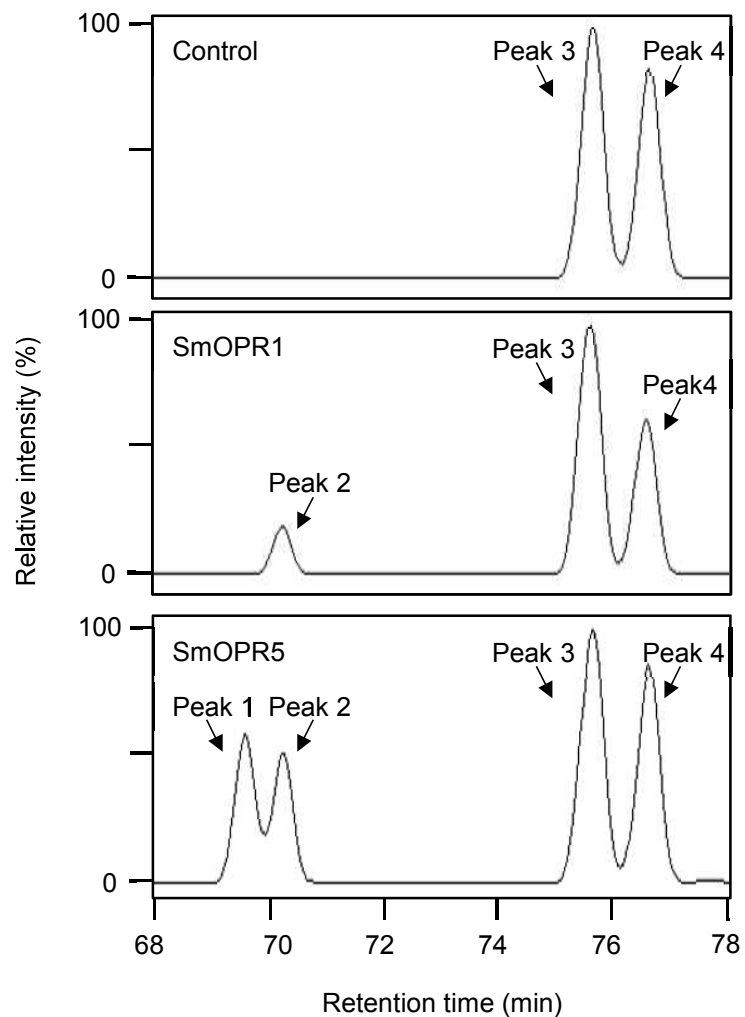


Fig. 7.

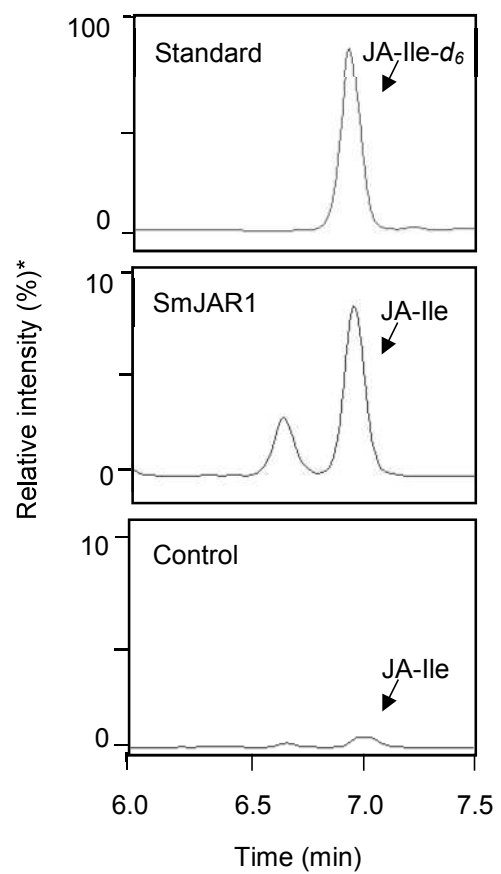


Fig. 8.

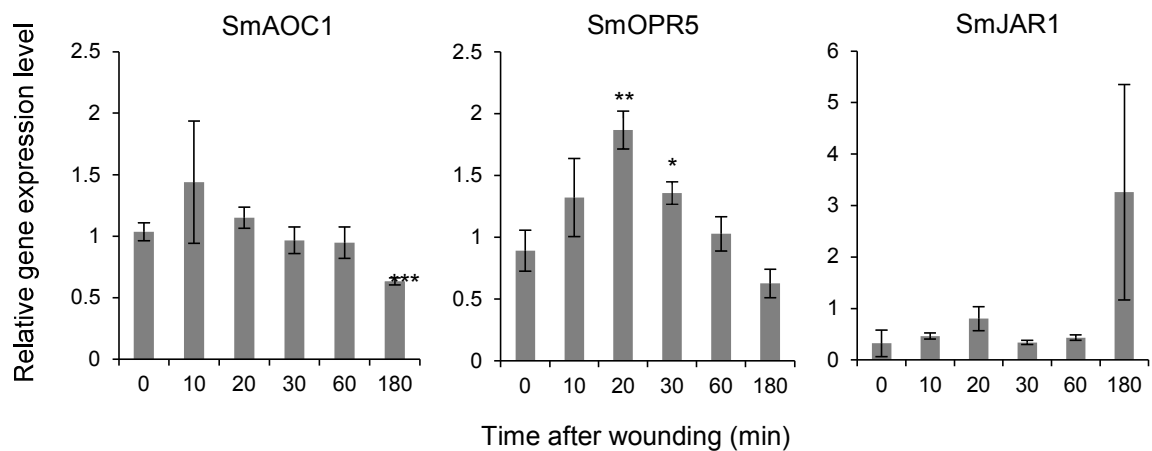


Fig. 9.

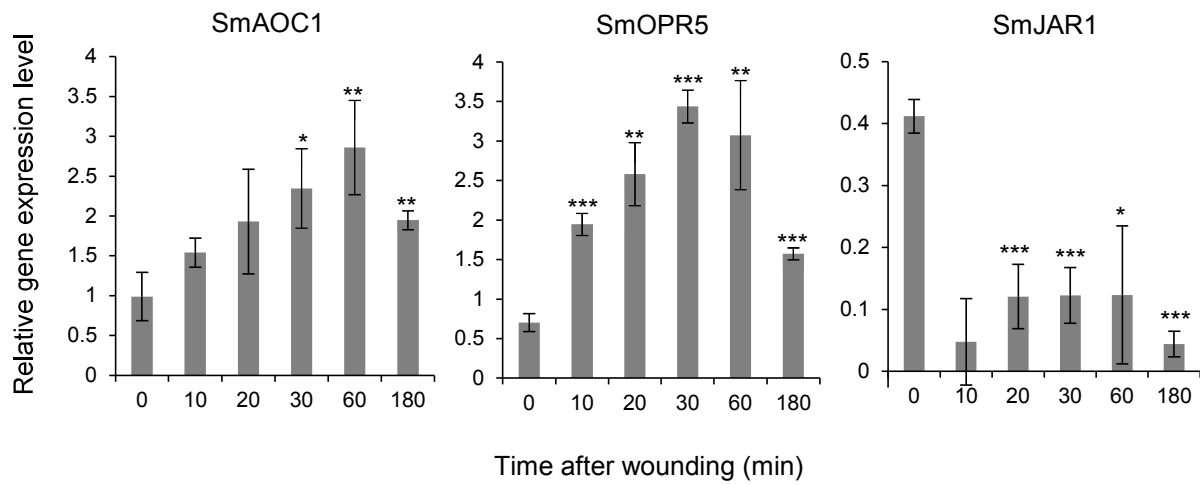


Fig. 10.

